Comprehensive identification of lysine 2-hydroxyisobutyrylated proteins in *Ustilaginoidea virens* reveals the involvement of lysine 2-hydroxyisobutyrylation in fungal virulence

Xiaoyang Chen[1], Xiabing Li[1], Pingping Li[1], Xiaolin Chen[1], Hao Liu[1], Junbin Huang[1], Chaoxi Luo[1], Tom Hsiang[2] and Lu Zheng[1]*

SUPPORTING INFORMATION

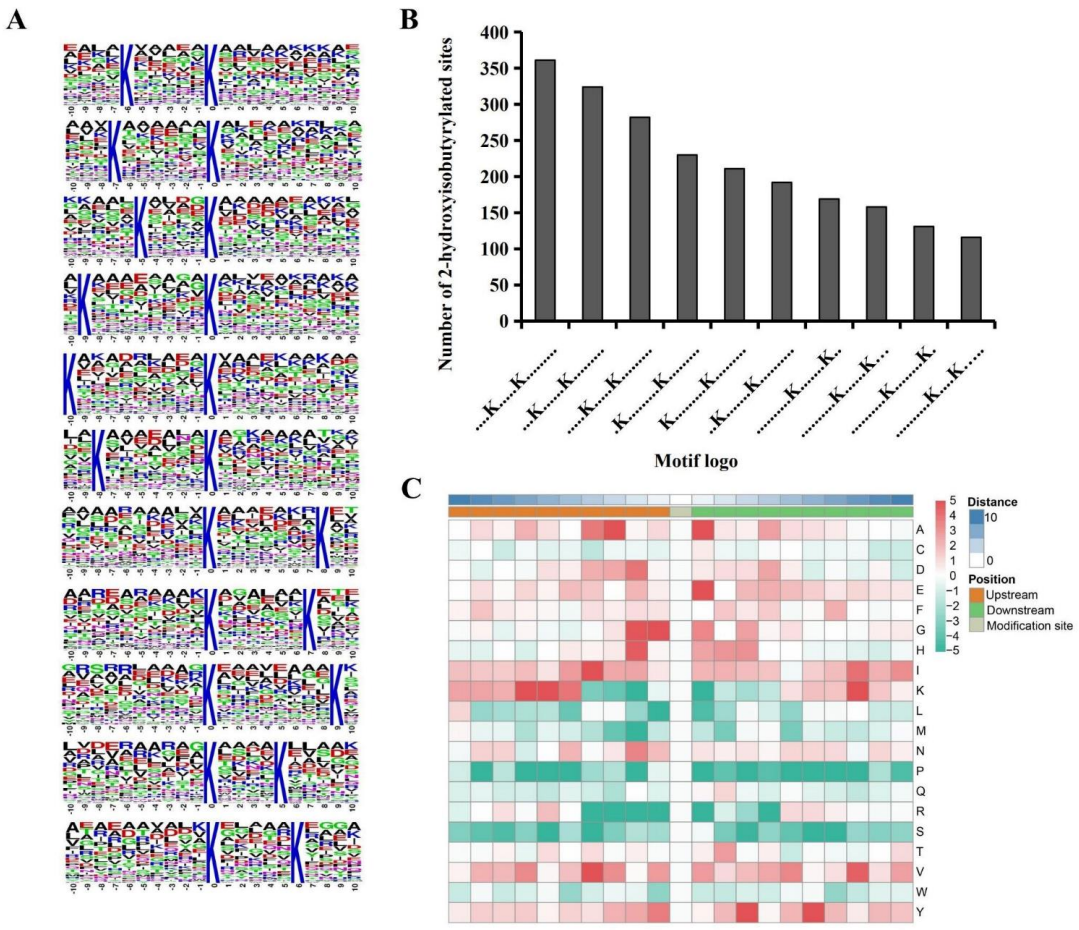

Figure S1. Consensus sequence analysis of all K_{hib} sites in *U. virens*

(**A**) Conserved motifs of 2-hydroxyisobutyryl-21-mers flanking the modification sites. The size of each letter is correlated with the frequency of that amino-acid residue occurring in that position. (**B**) Frequency of each motif occurring in the identified 2-hydroxyisobutyrylated peptides. (**C**) Heat map of the amino acid compositions around the 2-hydroxyisobutyrylation sites. The –log10 (Fisher's exact test *P* value) for every amino-acid in each position (from −10 to 10) is shown.

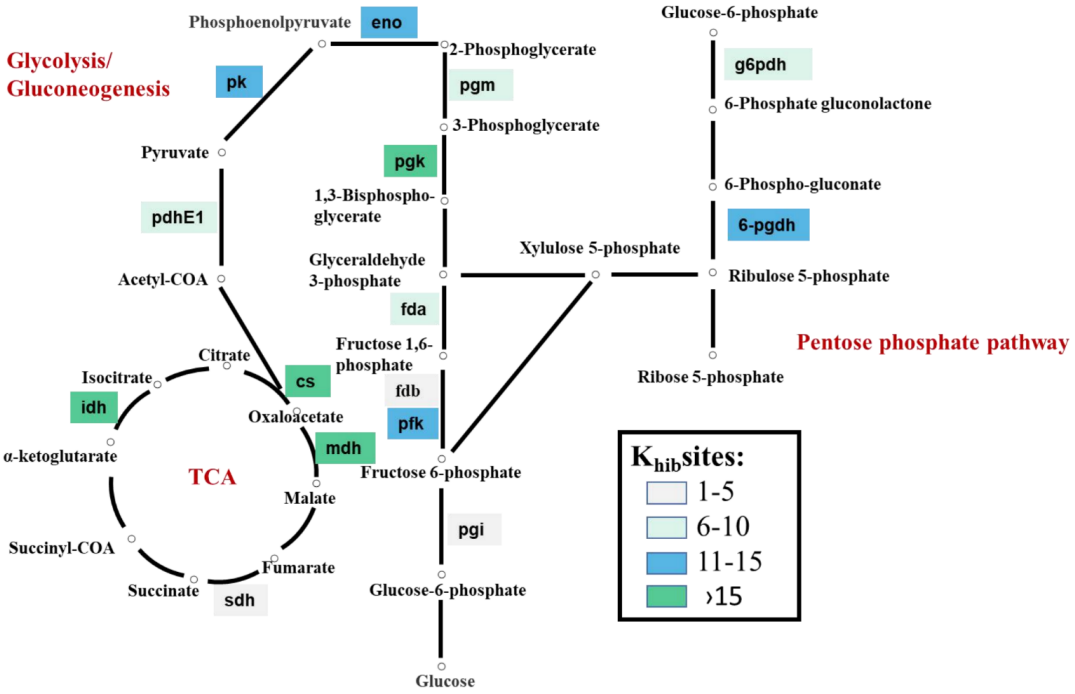

Figure S2. 2-hydroxyisobutyrylated enzymes in the central carbon metabolism network in *U. virens*

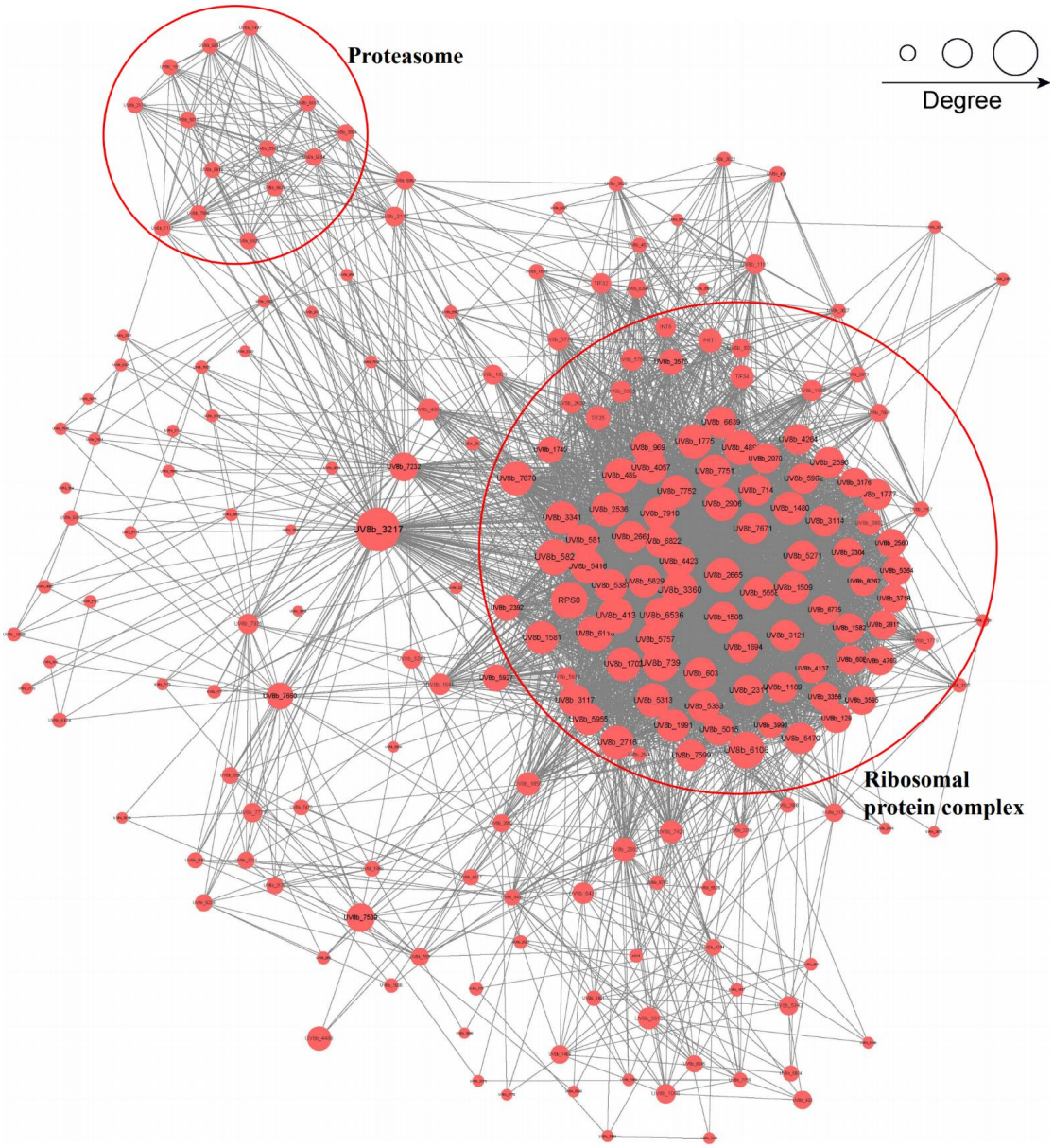

Figure S3. Interaction network of 2-hydroxyisobutyrylated proteins in *U. virens*

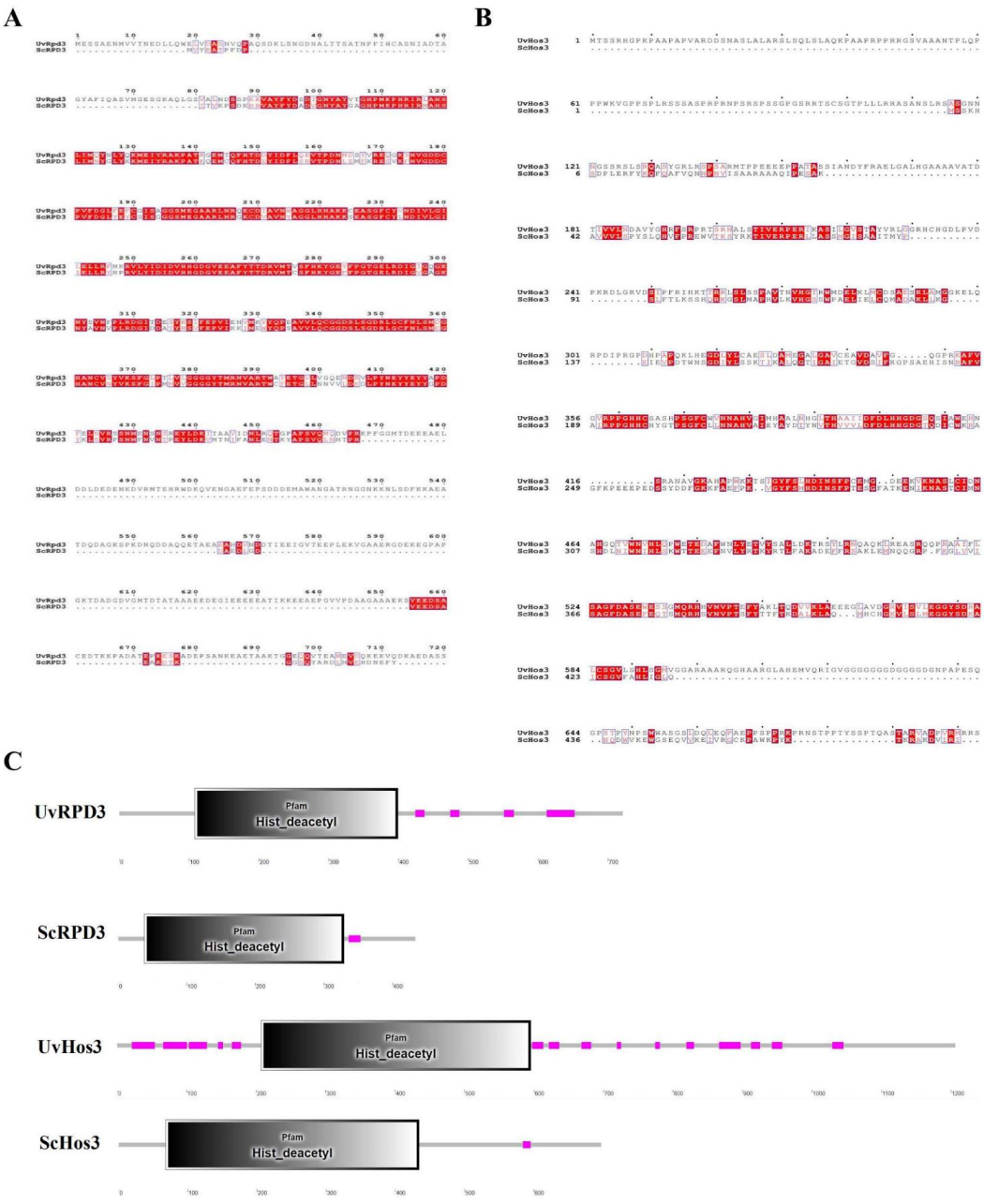

Figure S4. Homology analysis of Rpd3p and Hos3p in *S. cerevisiae* and *U. virens*

(**A**) Amino-acid sequence alignment of UvRpd3 and ScRpd3. Red highlights indicate the conserved regions of these proteins. (**B**) Amino-acid sequence alignment of UvHos3 and ScHos3. Red highlights indicate the conserved regions of these proteins. (**C**) Prediction of domains in UvRpd3, ScRpd3, UvHos3, and ScHos3. Black boxes depict the predicted Pfam domain of Hist_deacetyl in these proteins.

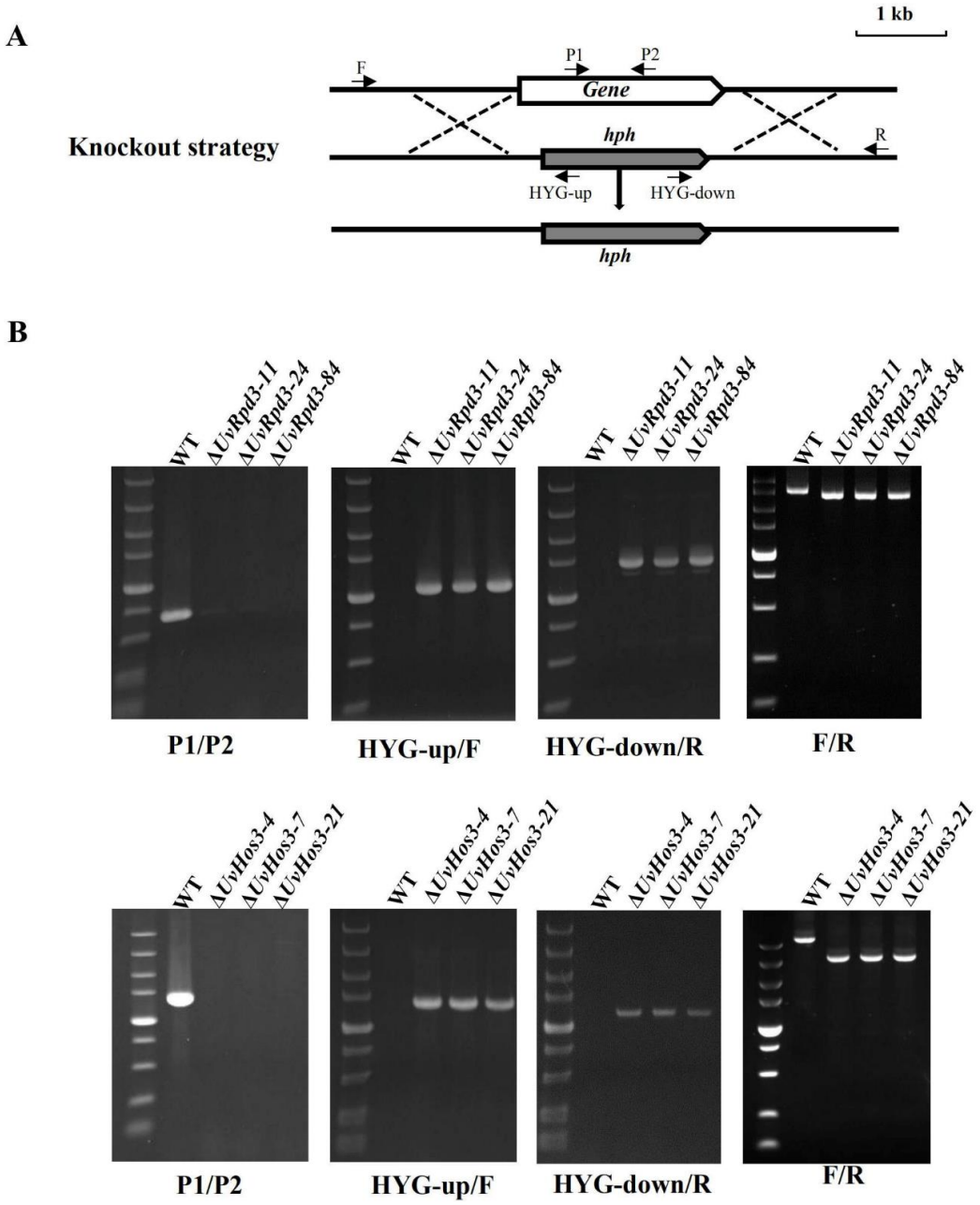

Figure S5. Deletion strategy for *UvRPD3* and *UvHos3* in *U. virens*

(**A**) Deletion strategy for targeted genes. Gene replacement of targeted genes through an ATMT approach. Genomic regions upstream and downstream of the targeted gene-coding sequence that was amplified and fused to segments of the hygromycin phosphotransferase (HYG) cassette. (**B**) PCR verification by amplifying the targeted genes using primer pair P1/P2 and the flanking sequences beside the replacement fragment by using primer pairs HYG-up/F and HYG-down/R in the transformants and

the wild-type strain (WT).

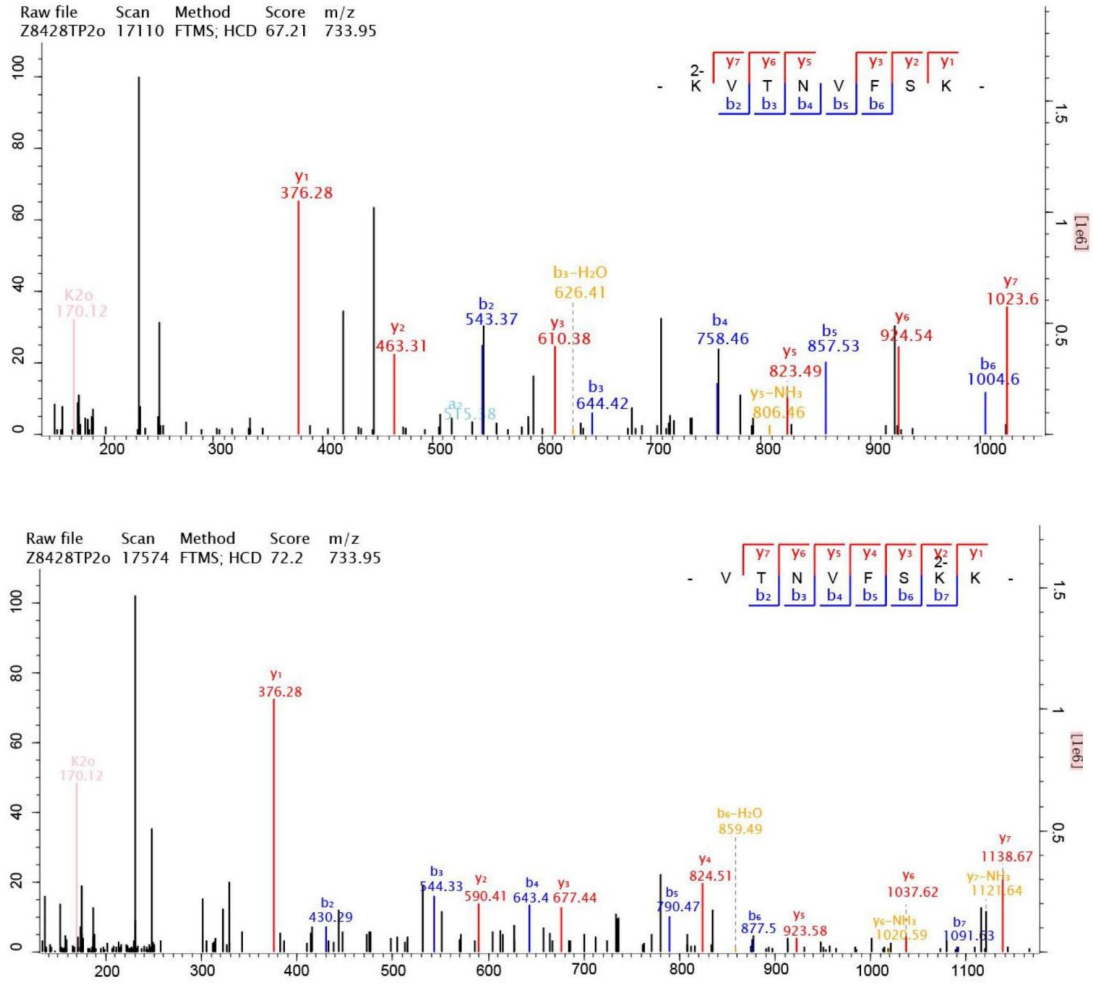

Figure S6. MS/MS spectrum of *in vivo* K_{hib} sites of UvSlt2

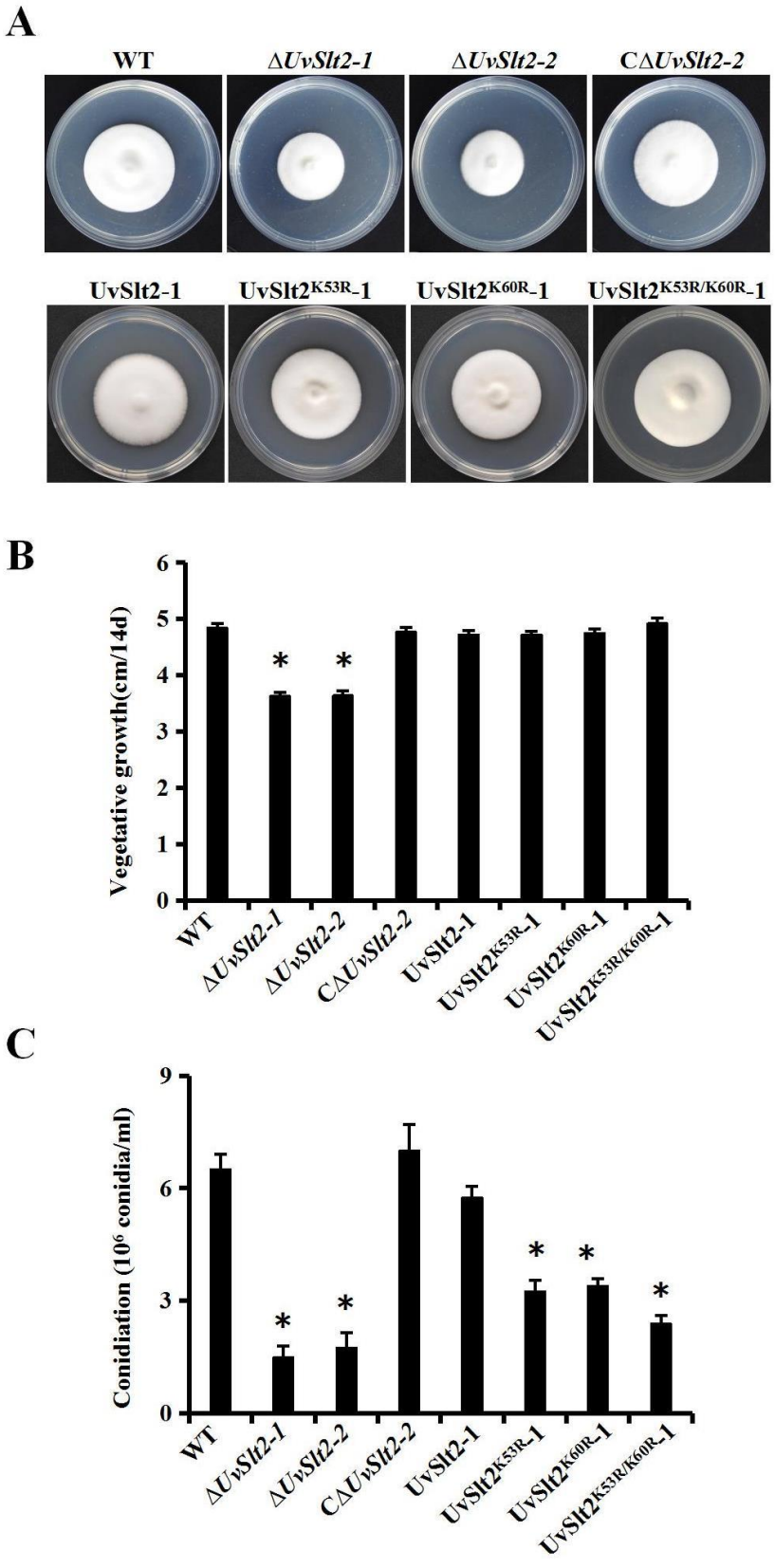

Figure S7. Defects of the *UvSlt2* mutants in growth and conidiation

(**A**) Colony morphology of the WT, the Δ*UvSlt2* deletion mutants and a

complementation strain, UvSlt2-1, and UvSlt2^{K53R}-1, UvSlt2^{K60R}-1, and UvSlt2$^{K53R/K60R}$-1 strains on PSA after 14 days of growth in darkness at 28 ℃. (**B**) Vegetative growth of the WT and mutants on PSA after 14 days in darkness at 28 ℃. (**C**) Conidial production of the WT and mutants after incubation in PSB at 28°C and 180 rpm for 7 days. Asterisks represent significant differences between the mutants and the WT by LSD at P=0.05.

Table S1. Modification site information of 2-hydroxyisobutyrylated proteins in *U. virens*

Table S2. Number of K_{hib} sites on diverse enzymes in *U. virens*

Table S3. Gene ontology classification of putative 2-hydroxyisobutyrylated proteins in *U. virens*

Table S4. KEGG pathway enrichment of 2-hydroxyisobutyrylated proteins in *U. virens*

Table S5. Primers used in this study